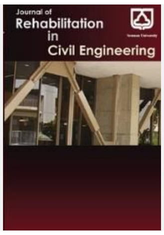

Journal of Rehabilitation in Civil Engineering

Journal homepage: https://civiljournal.semnan.ac.ir/

Influence of Semi-Rigid Connection Placement on the Static Stability of Steel Frames

Nguyen Hai Quang [1*]

1. Lecturer, Faculty of Mechanical-Automotive and Civil Engineering, Electric Power University, Ha Noi, Viet Nam

* Corresponding author: *quangnh@epu.edu.vn*

ARTICLE INFO

Article history:
Received: 22 July 2025
Revised: 09 September 2025
Accepted: 21 November 2025

Keywords:
semi-rigid connections;
steel frames;
connection layout;
geometric nonlinearity;
static stability;
finite element analysis.

ABSTRACT

In contemporary steel frame construction, semi-rigid joints are increasingly recognized for their ability to balance internal forces and limit stress concentrations. Most existing studies primarily focus on joints at beam–column intersections, while practical construction often introduces additional joints at mid-span when members are segmented and assembled on site. This research applies a finite element approach with geometric nonlinearity (P–Δ effect) to examine how the location of semi-rigid joints affects the static stability of planar steel frames. Both conventional end-joint configurations and alternative mid-span layouts are analyzed. The model, verified against benchmark results, is then used to explore variations in buckling load, deformation patterns, and moment distribution. The findings show that relocating joints to mid-span can enhance the critical load capacity by more than 230% in certain cases, emphasizing the structural significance of connection positioning. Based on these insights, practical recommendations are proposed for prefabricated steel structures with non-traditional connection arrangements.

E-ISSN: 2345-4423

How to cite this article:
Nguyen, H. Q. (2026). Influence of Semi-Rigid Connection Placement on the Static Stability of Steel Frames. (2393). Journal of Rehabilitation in Civil Engineering, 14(3), 2393 https://doi.org/10.22075/jrce.2025.2393

1. Introduction

1.1. Background of modern steel structure design and construction

In modern steel structure design, the connections between structural members, particularly between beams and columns, play a crucial role. They ensure the transfer of internal forces and establish the overall working mechanism of the frame system. In practice, most connections are neither perfectly rigid nor ideally pinned but fall into an intermediate state known as semi-rigid connections. This type of connection allows for partial moment transfer while still permitting a certain degree of relative rotation between members, enabling flexible internal force redistribution and reducing stress concentrations at the joints [1,2].

Over the past two decades, the application of semi-rigid connections has been increasingly encouraged due to their clear technical and economic advantages. Specifically, semi-rigid connections help optimize structural design, improve overall load-carrying capacity, and enhance construction efficiency [3,4]. Recent studies have also shown that these connections allow for the design of frames with better ductility and energy dissipation capacity, especially under seismic actions or cyclic loading conditions [5,6].

Notably, in the context of rapid development of prefabricated and pre-engineered buildings, it has become common practice to divide structural members into smaller segments for easier transportation and then assemble them on-site. This practice leads to the formation of internal joints at mid-span of beams or within the height of columns—non-traditional locations that were previously less considered in structural modeling [7–9]. However, these internal connections may significantly affect the overall stability and load-carrying resistance of the frame, especially when geometric nonlinearity effects are taken into account [10,11].

1.2. Gaps in the modeling and design of semi-rigid connections

Although the role of semi-rigid connections in steel structure design has been broadly acknowledged and adopted, the majority of current studies continue to concentrate on layouts where joints are assumed at beam–column intersections, essentially at member ends [3,12,13]. Previous studies focused on these end-joint connections because they are the main force-transfer locations and straightforward to model in commercial software [3,12]. However, this simplification neglects mid-span connections that are increasingly common in prefabricated frames [7,14], and their omission may critically affect stability, especially when geometric nonlinearity is considered [10,11].

1.3. Objectives and contributions of the study

This study aims to systematically evaluate the influence of semi-rigid connection placement on the static behavior and geometric stability of planar steel frames. The analysis is conducted using the finite element method with consideration of geometric nonlinearity (P–Delta effect). Unlike most previous studies that have been limited to traditional beam–column joint configurations [3,12,14], this research expands the scope by investigating two connection placement scenarios:

- ✓ Traditional configuration: joints assumed at the member ends (beam–column nodes);
- ✓ Non-traditional configuration: joints introduced at beam mid-span.

Figure 1 illustrates the fundamental difference between the two layouts: (a) connection at the structural joint, and (b) connection placed at mid-span of the beam.

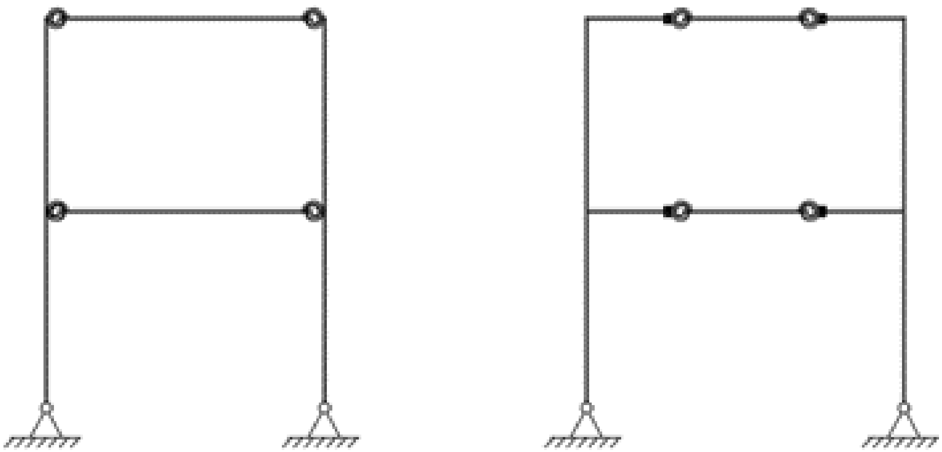

(a) (b)

Fig. 1. Two semi-rigid connection layout configurations. (a) Traditional configuration. (b) Non-traditional configuration.

In this study, a finite element formulation is proposed, allowing nonlinear semi-rigid joints to be assigned at arbitrary positions along members. The connection moment–rotation behavior is represented by two well-established models: the Kishi–Chen three-parameter formulation and the Richard–Abbott four-parameter model. These models allow for accurate simulation of real-world connection behaviors in bolted, angle cleat, or partial penetration welded connections.

In addition to developing a new finite element formulation, the study employs a dual-analysis approach: on the one hand, a custom simulation program is developed using MATLAB to provide full control over the calculation process and model calibration; on the other hand, the commercial software SAP2000 is used for cross-verification of results and to enhance practical applicability. This combination improves the reliability of the results and extends the applicability of the study to real-world structural design scenarios [4,11,15].

1.4. Key contributions

This study makes several notable contributions to the field of steel structures, as summarized below:

- ✓ Development of a finite element model capable of simulating nonlinear semi-rigid connections at non-traditional locations along the length of beams and columns—an approach that has not been thoroughly addressed in previous studies [7,9,14].
- ✓ Integration of two analytical tools: a custom-built MATLAB model and the commercial software SAP2000. This dual approach not only enhances the reliability of the analytical results but also enables cross-validation of the model under various boundary conditions and connection configurations [11,15,16].
- ✓ This study provides an in-depth examination of how joint positioning affects the main mechanical responses of steel frames, such as force redistribution, displacement, rotational behavior, and the critical load linked to geometric instability [1,10,11,17].
- ✓ Design recommendations with practical applications for prefabricated buildings such as industrial facilities, pre-engineered steel structures, or modular frames that require segmentation for transportation. The results provide technical justification for adjusting connection placement to achieve better structural stability and construction economy in field-assembled conditions [4,7,8,18].

2. Related research

2.1. Influence of semi-rigid joints on the behavior of steel frames

Recent studies continue to affirm the critical role of semi-rigid joints in governing the stiffness, force redistribution, and overall stability of steel frames. Advances in analytical and experimental research have shown that the mechanical response of frames is highly sensitive to the rotational stiffness of joints and to the way these joints are represented in numerical models. Most existing investigations, however, remain focused on traditional beam–column intersections, with limited attention given to non-traditional internal joints formed during prefabrication or segmented assembly. This gap highlights the need to reassess how connection placement—whether at member ends or along the span—influences global behavior, particularly when geometric nonlinearity is considered.

Since the late 20th century, semi-rigid joints have attracted significant attention in steel structure research. Unlike the two idealized types—perfectly pinned and fully rigid—semi-rigid connections are capable of transmitting a portion of bending moments while still allowing for relative rotation between members. This makes them more practical for real construction scenarios, particularly in structures employing bolted joints, angle cleats, partial welds, or prefabricated components [1,12,16,17].

Recent experimental and numerical studies have shown that semi-rigid connections significantly influence the mechanical behavior of steel frames in both serviceability and ultimate limit states. Reducing the rotational stiffness at joints alters the distribution of bending moments along beams and columns, thereby affecting internal forces, deformations, and stress distribution across the structure [3,6,16]. Semi-rigid connections also increase the overall flexibility of the frame, helping to reduce stress concentration at joints—often the weakest point in design and construction—and enhance energy dissipation capacity [4,5,7,8].

When subjected to lateral actions such as wind or earthquakes, or when second-order geometric nonlinearity (commonly known as the P–Δ phenomenon) is included, the existence of semi-rigid joints may considerably change the structural response mechanisms [1,10,11]. Some studies also indicate that properly placed semi-rigid connections may influence the natural frequencies of the structure, potentially improving dynamic performance [4,5].

2.2. Moment–rotation models and nonlinear formulations

One of the key technical challenges in modeling semi-rigid connections is accurately characterizing the nonlinear moment–rotation (M–θ) relationship, which depends on the actual connection type. Various empirical formulations have been proposed to capture this behavior, with two of the most commonly applied being the Kishi–Chen three-parameter model [9] and the Richard–Abbott four-parameter model [1].

The Kishi–Chen approach [9] characterizes the M–θ relationship using three key parameters—initial stiffness, ultimate moment capacity, and a curve-shaping coefficient—allowing it to approximate a progressively increasing moment–rotation curve. Its advantages include simplicity and ease of calibration, while still offering accurate representation of angle cleat connections, particularly in the elastic and early hardening stages [9]. This model is commonly used in planar frame simulations with simple semi-rigid joints [3,12].

By contrast, the Richard–Abbott model [1] employs four parameters and provides a more comprehensive depiction of three regions: linear elastic, nonlinear hardening, and plastic deformation—suitable for joints subjected to large deformations or cyclic loading. Due to its flexible calibration capabilities, this model is often used in advanced nonlinear analyses, particularly for space frames or dynamic loading conditions [1,5,6].

Both models have been effectively applied in recent studies involving nonlinear finite element simulations of semi-rigid connections [1,9,11]. The choice between them depends on the connection configuration, analysis requirements, and the deformation range being modeled.

2.3. Current modeling and analysis methods

When analyzing structural systems that include semi-rigid joints, two primary modeling strategies are commonly adopted:

Rotational spring elements at joints: This is the most common method, especially in commercial software such as SAP2000 and ETABS. The semi-rigid behavior is modeled by assigning an equivalent rotational stiffness at the member ends, simplifying the modeling process and allowing for convenient force control [3,13]. However, this method only supports joint-end connections and is not suitable for internal connections located at mid-span or within the member height.

Integrated finite elements with internal semi-rigid behavior: This approach allows for direct incorporation of nonlinear moment–rotation (M–θ) behavior within the element itself, and can also account for second-order geometric effects (P–Delta) when necessary. It offers greater flexibility and accuracy in simulating real-world connections, particularly useful for custom-built models used in verification studies [1,11].

Recently, some studies have adopted a hybrid modeling approach: using commercial software to build the overall model and perform preliminary analysis, while simultaneously developing MATLAB or Python programs for verification, nonlinear parameter calibration, or sensitivity studies [4,7,15]. This strategy leverages the speed and intuitive interface of commercial tools alongside the flexibility and extensibility of in-house models.

Nevertheless, most current studies still assume that semi-rigid connections are only placed at the member ends—that is, at the structural joints. This leads to a major limitation in representing real construction conditions, where internal connections may be located at mid-span or mid-height due to segmentation for transportation and assembly [7,8,14]. To date, there are very few models capable of simulating nonlinear connections at arbitrary positions along the member length with sufficient accuracy for design applications [10,11].

2.4. Research gaps

A review of studies from the past two decades reveals a clear research gap: most work on semi-rigid connections focuses on rotational stiffness characteristics or moment–rotation models, while the influence of connection placement along members—especially at non-traditional locations like beam mid-spans or column mid-heights—has not been adequately investigated [7,8,14].

In practical construction, the need to transport and assemble components on site makes segmentation of beams and columns increasingly common. This results in a growing prevalence of internal semi-rigid joints—a configuration not accounted for in traditional structural models, which assume connections only at the nodes. Changes in connection placement can significantly affect internal force distribution, stress patterns, and geometric stability mechanisms of the entire system, particularly in nonlinear analyses involving the P–Delta effect or critical load evaluations [2,10,11].

Although some recent studies have addressed nonlinear behavior and incorporated empirical connection models into finite element formulations [1,9,12], there is still a lack of analytical models that simultaneously:

- ✓ Accurately simulate nonlinear semi-rigid connections at arbitrary locations along the member length;

- ✓ Incorporate second-order geometric nonlinearity (P–Δ) to accurately represent the real buckling response of frame structures;
- ✓ Allow cross-verification using different modeling tools to ensure reliability and practical applicability.

This gap underscores the urgent need for more flexible analytical models that serve modern design requirements, particularly for prefabricated structures where connection placement can significantly enhance structural stability and economic efficiency. Addressing this challenge is the central objective of the present study.

3. Research methodology

3.1. Frame models and connection layout scenarios

In this study, planar steel frame models are developed with typical configurations consisting of two stories and one or two spans. The models use beam–column elements with constant cross-sectional and material properties. The frame behavior is assumed to be planar, and all materials are modeled as linearly elastic. The connections between members are represented by two semi-rigid connection placement scenarios:

Scenario 1: Joints assumed to be semi-rigid at the beam–column ends (traditional layout);

Scenario 2: Semi-rigid joints placed at beam mid-spans or column mid-heights (non-traditional arrangement).

Figure 2 illustrates a general schematic of the frame model that can incorporate all connection placement scenarios. It is important to note that this is a conceptual diagram and does not represent specific numerical examples used in the later sections. The elements are numbered to designate the locations of the connections, with different mechanical properties assigned based on each scenario.

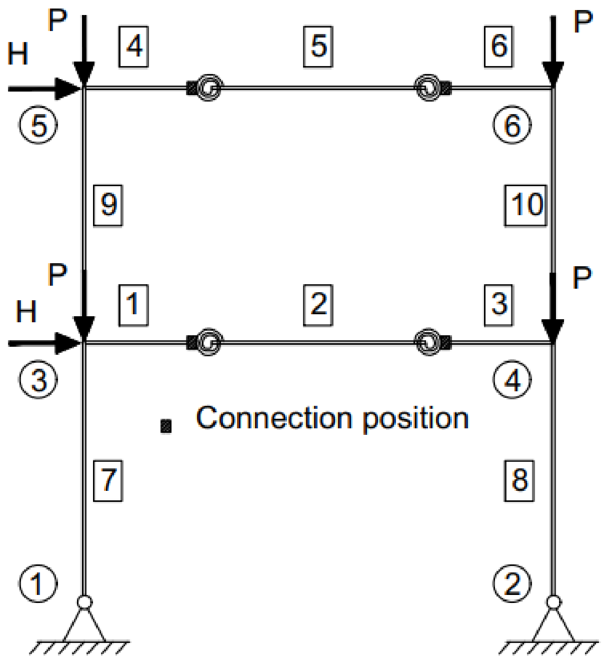

Fig. 2. Model of a two-story, one-bay steel frame showing potential locations of semi-rigid connections.

A two-dimensional frame model was adopted in order to isolate the in-plane behavior and clearly evaluate the influence of semi-rigid connection placement on static stability. Extension to three-dimensional frames will be considered in future work.

3.2. Nonlinear semi-rigid connection element model

To simulate semi-rigid connections, the study employs beam elements with two ends, capable of assigning nonlinear moment–rotation relationships at desired positions. The element formulation accounts for geometric nonlinearity (P–Δ effect) and follows the concept of beam–column elements, where the formulation employs a linear elastic stiffness matrix together with a geometric stiffness matrix obtained from the strain energy principle [1,2,11].

Figure 3 shows the beam–column element formulation incorporating nonlinear semi-rigid joints and the geometric P–Δ effect (adapted from [9]), together with the notation used for internal forces, displacements, and rotations. Let the e^{th} beam–column element have end connections A and B modeled as elastic rotational springs, thereby representing a semi-rigid member. The local coordinate system Oxy is defined such that the x-axis follows the element's longitudinal direction, the y-axis is oriented upward and perpendicular to it, and the origin is placed at node A. The parameters A, I, L, and E denote, respectively, the cross-sectional area, moment of inertia, span length, and Young's modulus of the material. At the i^{th} load increment, N_A, Q_A, and M_A indicate the axial force along the x-axis, the shear force along the y-axis, and the bending moment about the z-axis at end A; correspondingly, N_B, Q_B, and M_B refer to the same quantities at end B.

The axial and transverse displacements at nodes A and B are denoted by u_A, v_A, and u_B, v_B , respectively. Rotations of the frame nodes about the z-axis are represented by θ_A and θ_B, whereas the beam-end rotations are indicated as θ_{eA} and θ_{eB}. The connection rotations at nodes A and B are expressed as θ_{cA} and θ_{cB}, and the corresponding rotational stiffness values are k_A and k_B.

Figure 3 shows the kinematic relations among displacement, internal force, and deformation for an element with a semi-rigid joint. In this model, the joint is assumed dimensionless, the influence of axial and shear forces on joint action is neglected, the member material is treated as linearly elastic, and the beam behavior is described by the Euler–Bernoulli assumption. The connection's moment–rotation law may be linear, piecewise-linear, or nonlinear.

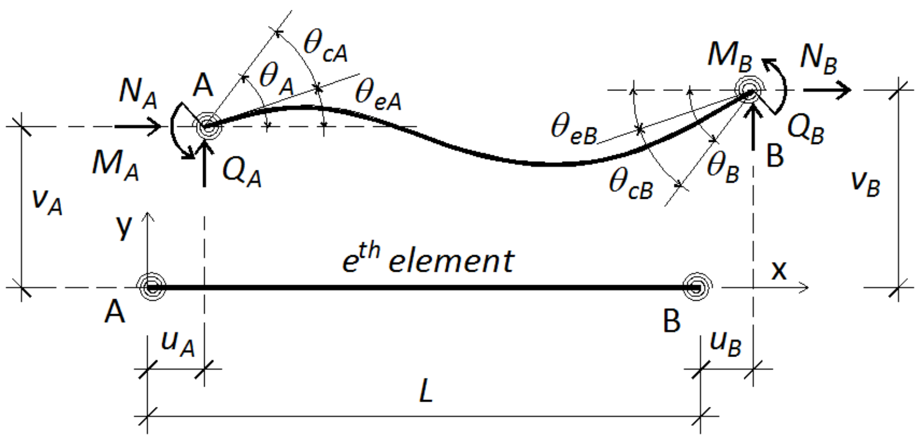

Fig. 3. Beam–column element formulation incorporating nonlinear semi-rigid joints and the geometric (P–Δ) effect (adapted from [9]).

3.2.1. Modeling of semi-rigid joints

Although joints may undergo different types of deformation (such as axial, shear, flexural, or torsional), this study focuses only on bending behavior. The mechanical response of a connection is represented by its moment–rotation relationship. Numerous mathematical formulations have been proposed to capture this response, and experimental evidence confirms that it is inherently nonlinear. For computational convenience, simplified linear or piecewise-linear models are often adopted. In the present work, three approaches are applied in the case studies: a linear model, the Kishi–Chen three-parameter exponential model [2], and the Richard–Abbott four-parameter exponential model [2], corresponding to Examples 1, 2, and 3.

The three-parameter power model proposed by Kishi-Chen [2], includes three parameters: initial connection stiffness k_0, ultimate connection moment capacity M_u and shape parameter n, as follows:

$$M = \frac{k_0\theta}{\left[1+\left(\frac{\theta}{\theta_0}\right)^n\right]^{\frac{1}{n}}} \tag{1}$$

In this expression, M denotes the moment and θ represents the rotation angle at the considered load step of the joint. The term $\theta_0 = M_u/k_0$ is defined as the reference plastic rotation, and the tangent stiffness of the connection is expressed as [2]:

$$\mathrm{k} = \frac{\mathrm{dM}}{\mathrm{d\theta}} = \frac{\mathrm{k_0}}{\left[1+\left(\frac{\theta}{\theta_0}\right)^{\mathrm{n}}\right]^{\frac{(\mathrm{n}+1)}{\mathrm{n}}}} \tag{2}$$

The exponential model with four parameters, introduced by Richard–Abbott [2], is characterized by: the initial stiffness k_0, the strain-hardening stiffness k_p, the reference moment M_0, and a curve-shaping coefficient n. The mathematical expression of this model can be written as [2]:

$$\mathrm{M} = \frac{(\mathrm{k_0}-\mathrm{k_p})|\theta|}{\left[1+\left|\frac{(\mathrm{k_0}-\mathrm{k_p})|\theta|}{\mathrm{M_0}}\right|^{\mathrm{n}}\right]^{\frac{1}{\mathrm{n}}}} + \mathrm{k_p}|\theta| \tag{3}$$

and the tangent stiffness associated with the connection can be expressed as [2]:

$$\mathrm{k} = \left.\frac{\mathrm{dM}}{\mathrm{d\theta}}\right|_{|\theta|=|\theta|} = \frac{(\mathrm{k_0}-\mathrm{k_p})}{\left[1+\left|\frac{(\mathrm{k_0}-\mathrm{k_p})|\theta|}{\mathrm{M_0}}\right|^{\mathrm{n}}\right]^{\frac{\mathrm{n}+1}{\mathrm{n}}}} + \mathrm{k_p} \tag{4}$$

Among various moment–rotation models proposed in the literature, the Kishi–Chen and Richard–Abbott formulations were selected because they are widely validated, require relatively simple calibration parameters, and provide complementary capabilities: the Kishi–Chen model is efficient for typical semi-rigid joints, while the Richard–Abbott model captures nonlinear hardening and large-rotation effects essential for advanced nonlinear analysis.

3.2.2. Formulation of the stiffness matrix for elements with semi-rigid joints [9]

The stiffness matrix of the element can be written as:

$$[\mathrm{k_s}]_\mathrm{e} = [\mathrm{k_{L-Es}}]_\mathrm{e} + [\mathrm{k_{Gs}}]_\mathrm{e} \tag{5}$$

which corresponds to the case where the element has semi-rigid joints at both ends. In this expression,

$$[\mathrm{k_{L-Es}}]_\mathrm{e} = [\mathrm{k_{Es}}]_\mathrm{e} + [\mathrm{k_{Cs}}]_\mathrm{e} \tag{6}$$

where $[k_{Es}]_e$ denotes the linear elastic stiffness matrix of the element itself, and $[k_{Cs}]_e$ represents the linear elastic stiffness contribution of the connections.

$$[\mathrm{k_{Es}}]_\mathrm{e} = \begin{bmatrix} \mathrm{k_{Es}^{1,1}} & 0 & 0 & \mathrm{k_{Es}^{1,4}} & 0 & 0 \\ 0 & \mathrm{k_{Es}^{2,2}} & \mathrm{k_{Es}^{2,3}} & 0 & \mathrm{k_{Es}^{2,5}} & \mathrm{k_{Es}^{2,6}} \\ 0 & \mathrm{k_{Es}^{3,2}} & \mathrm{k_{Es}^{3,3}} & 0 & \mathrm{k_{Es}^{3,5}} & \mathrm{k_{Es}^{3,6}} \\ \mathrm{k_{Es}^{4,1}} & 0 & 0 & \mathrm{k_{Es}^{4,4}} & 0 & 0 \\ 0 & \mathrm{k_{Es}^{5,2}} & \mathrm{k_{Es}^{5,3}} & 0 & \mathrm{k_{Es}^{5,5}} & \mathrm{k_{Es}^{5,6}} \\ 0 & \mathrm{k_{Es}^{6,2}} & \mathrm{k_{Es}^{6,3}} & 0 & \mathrm{k_{Es}^{6,5}} & \mathrm{k_{Es}^{6,6}} \end{bmatrix} \tag{7}$$

wherein:

$k_{Cs}^{2,2} = 36E^2I^2\left(\frac{d_2^2}{k_A} + \frac{d_8^2}{k_B}\right)$

$k_{Cs}^{2,3} = k_{Cs}^{3,2} = 12E^2I^2\left(\frac{d_2d_5}{k_A} + \frac{d_7d_8}{k_B}\right)$

$k_{Cs}^{2,5} = k_{Cs}^{5,2} = -36E^2I^2\left(\frac{d_2^2}{k_A} + \frac{d_8^2}{k_B}\right)$

$k_{Cs}^{2,6} = k_{Cs}^{6,2} = 12E^2I^2\left(\frac{d_2d_7}{k_A} + \frac{d_8d_9}{k_B}\right)$

$k_{Cs}^{3,3} = 4E^2I^2\left(\frac{d_5^2}{k_A} + \frac{d_7^2}{k_B}\right)$

$k_{Cs}^{3,5} = k_{Cs}^{5,3} = -12E^2I^2\left(\frac{d_2d_5}{k_A} + \frac{d_7d_8}{k_B}\right)$

$k_{Cs}^{3,6} = k_{Cs}^{6,3} = 4E^2I^2\left(\frac{d_5d_7}{k_A} + \frac{d_7d_9}{k_B}\right)$

$k_{Cs}^{5,5} = 36E^2I^2\left(\frac{d_2^2}{k_A} + \frac{d_8^2}{k_B}\right)$

$k_{Cs}^{5,6} = k_{Cs}^{6,5} = -12E^2I^2\left(\frac{d_2d_7}{k_A} + \frac{d_8d_9}{k_B}\right)$

$k_{Cs}^{6,6} = 4E^2I^2\left(\frac{d_7^2}{k_A} + \frac{d_9^2}{k_B}\right)$

The entries of the elastic stiffness matrix $[k_{L-Es}]_e$ in Eq. (6) can be expressed as

$$[\mathrm{k}_{\mathrm{L-Es}}]_{\mathrm{e}} = \begin{bmatrix} \mathrm{k}_{\mathrm{L-Es}}^{1,1} & 0 & 0 & \mathrm{k}_{\mathrm{L-Es}}^{1,4} & 0 & 0 \\ 0 & \mathrm{k}_{\mathrm{L-Es}}^{2,2} & \mathrm{k}_{\mathrm{L-Es}}^{2,3} & 0 & \mathrm{k}_{\mathrm{L-Es}}^{2,5} & \mathrm{k}_{\mathrm{L-Es}}^{2,6} \\ 0 & \mathrm{k}_{\mathrm{L-Es}}^{3,2} & \mathrm{k}_{\mathrm{L-Es}}^{3,3} & 0 & \mathrm{k}_{\mathrm{L-Es}}^{3,5} & \mathrm{k}_{\mathrm{L-Es}}^{3,6} \\ \mathrm{k}_{\mathrm{L-Es}}^{4,1} & 0 & 0 & \mathrm{k}_{\mathrm{L-Es}}^{4,4} & 0 & 0 \\ 0 & \mathrm{k}_{\mathrm{L-Es}}^{5,2} & \mathrm{k}_{\mathrm{L-Es}}^{5,3} & 0 & \mathrm{k}_{\mathrm{L-Es}}^{5,5} & \mathrm{k}_{\mathrm{L-Es}}^{5,6} \\ 0 & \mathrm{k}_{\mathrm{L-Es}}^{6,2} & \mathrm{k}_{\mathrm{L-Es}}^{6,3} & 0 & \mathrm{k}_{\mathrm{L-Es}}^{6,5} & \mathrm{k}_{\mathrm{L-Es}}^{6,6} \end{bmatrix} \tag{8}$$

where: $k_{L-Es}^{\eta,\kappa} = k_{Es}^{\eta,\kappa} + k_{Cs}^{\eta,\kappa}$, for $\eta = 1 \div 6$ and $\kappa = 1 \div 6$.

The geometric stiffness matrix corresponding to the semi-rigid beam–column element can be expressed as:

$$[\mathrm{k}_{\mathrm{Gs}}]_{\mathrm{e}} = \mathrm{N}\begin{bmatrix} 0 & 0 & 0 & 0 & 0 & 0 \\ 0 & \mathrm{k}_{\mathrm{Gs}}^{2,2} & \mathrm{k}_{\mathrm{Gs}}^{2,3} & 0 & \mathrm{k}_{\mathrm{Gs}}^{2,5} & \mathrm{k}_{\mathrm{Gs}}^{2,6} \\ 0 & \mathrm{k}_{\mathrm{Gs}}^{3,2} & \mathrm{k}_{\mathrm{Gs}}^{3,3} & 0 & \mathrm{k}_{\mathrm{Gs}}^{3,5} & \mathrm{k}_{\mathrm{Gs}}^{3,6} \\ 0 & 0 & 0 & 0 & 0 & 0 \\ 0 & \mathrm{k}_{\mathrm{Gs}}^{5,2} & \mathrm{k}_{\mathrm{Gs}}^{5,3} & 0 & \mathrm{k}_{\mathrm{Gs}}^{5,5} & \mathrm{k}_{\mathrm{Gs}}^{5,6} \\ 0 & \mathrm{k}_{\mathrm{Gs}}^{6,2} & \mathrm{k}_{\mathrm{Gs}}^{6,3} & 0 & \mathrm{k}_{\mathrm{Gs}}^{6,5} & \mathrm{k}_{\mathrm{Gs}}^{6,6} \end{bmatrix} \tag{9}$$

wherein:

$k_{Gs}^{2,2} = d_1^2L + 6d_1d_2L^2 - 2d_1d_3L^3 + 12d_2^2L^3 - 9d_2d_3L^4 + \frac{9}{5}d_3^2L^5$

$k_{Gs}^{2,3} = k_{Gs}^{3,2} = \Big(-d_1d_2L^3 - d_1d_4L + d_1d_5L^2 - \frac{9}{2}d_2^2L^4 + \frac{9}{5}d_2d_3L^5 - 3d_2d_4L^2 + 4d_2d_5L^3 + d_3d_4L^3 -$
$\frac{3}{2}d_3d_5L^4\Big)$

$k_{Gs}^{2,5} = k_{Gs}^{5,2} = -d_1^2L - 6d_1d_2L^2 + 2d_1d_3L^3 - 12d_2^2L^3 + 9d_2d_3L^4 - \frac{9}{5}d_3^2L^5$

$k_{GS}^{2,6} = k_{GS}^{6,2} = \left(d_1 d_6 L + d_1 d_7 L^2 - d_1 d_8 L^3 + 3d_2 d_6 L^2 + 4d_2 d_7 L^3 - \frac{9}{2} d_2 d_8 L^4 - d_3 d_6 L^3 - \frac{3}{2} d_3 d_7 L^4 + \frac{9}{5} d_3 d_8 L^5\right)$

$k_{GS}^{3,3} = \frac{9}{5} d_2^2 L^5 + 2d_2 d_4 L^3 - 3d_2 d_5 L^4 + d_4^2 L - 2d_4 d_5 L^2 + \frac{4}{3} d_5^2 L^3$

$k_{GS}^{3,5} = k_{GS}^{5,3} = \left(d_1 d_2 L^3 + d_1 d_4 L - d_1 d_5 L^2 + \frac{9}{2} d_2^2 L^4 - \frac{9}{5} d_2 d_3 L^5 + 3d_2 d_4 L^2 - 4d_2 d_5 L^3 - d_3 d_4 L^3 + \frac{3}{2} d_3 d_5 L^4\right)$

$k_{GS}^{3,6} = k_{GS}^{6,3} = \left(-d_2 d_6 L^3 - \frac{3}{2} d_2 d_7 L^4 + \frac{9}{5} d_2 d_8 L^5 + d_4 d_6 L - d_4 d_7 L^2 + d_4 d_8 L^3 + d_5 d_6 L^2 + \frac{4}{3} d_5 d_7 L^3 - \frac{3}{2} d_5 d_8 L^4\right)$

$k_{GS}^{5,5} = d_1^2 L + 6d_1 d_2 L^2 - 2d_1 d_3 L^3 + 12 d_2^2 L^3 - 9 d_2 d_3 L^4 + \frac{9}{5} d_3^2 L^5$

$k_{GS}^{5,6} = k_{GS}^{6,5} = \left(-d_1 d_6 L - d_1 d_7 L^2 + d_1 d_8 L^3 - 3d_2 d_6 L^2 - 4d_2 d_7 L^3 + \frac{9}{2} d_2 d_8 L^4 + d_3 d_6 L^3 + \frac{3}{2} d_3 d_7 L^4 - \frac{9}{5} d_3 d_8 L^5\right)$

$k_{GS}^{6,6} = d_6^2 L + 2d_6 d_7 L^2 - 2d_6 d_8 L^3 + \frac{4}{3} d_7^2 L^3 - 3d_7 d_8 L^4 + \frac{9}{5} d_8^2 L^5$

$d_0 = 12E^2 I^2 + 4EILk_A + 4EILk_B + L^2 k_A k_B$

$d_1 = \frac{6EI(2EI + Lk_B)}{Ld_0}$; $d_2 = \frac{(2EI + Lk_B)k_A}{Ld_0}$; $d_3 = \frac{2(EIk_A + EIk_B + Lk_A k_B)}{L^2 d_0}$; $d_4 = \frac{L(4EI + Lk_B)k_A}{d_0}$;

$d_5 = \frac{2(3EI + Lk_B)k_A}{d_0}$; $d_6 = \frac{2LEIk_B}{d_0}$; $d_7 = \frac{Lk_A k_B}{d_0}$; $d_8 = \frac{(2EI + Lk_A)k_B}{Ld_0}$

wherein:

E: Modulus of Elasticity of the material (typically steel);

I: Moment of inertia of the beam's cross-section with respect to its neutral axis;

L: Span length of the beam;

k_A, k_B: Rotational stiffness of the semi-rigid connections at ends A and B of the beam.

3.3. Analysis method and software tools

This research applies nonlinear static analysis to rigorously assess how the positioning of semi-rigid joints affects the distribution of internal forces, deformation behavior, and overall geometric stability of steel frames. For comparison, linear analysis is also carried out in certain cases, emphasizing the importance of including geometric nonlinearity in the modeling process.

Two computational tools are employed in the simulation and analysis process:

- ✓ SAP2000 – a commercial software specialized for structural analysis, which allows for assigning elastic connections at joints and provides convenient control over internal forces and deformation shapes [3,15].
- ✓ MATLAB – used to develop custom simulation code with user-defined element stiffness matrices, enabling independent result verification and flexible model parameter calibration [4,11].

The input parameters of the models include:

Structural geometry: story height, span length, and beam segment lengths;

- ✓ Material parameter: Young's modulus E;
- ✓ Sectional properties: area A and moment of inertia I of the members;
- ✓ Connection stiffness: represented by the M–θ moment–rotation models described above.

The evaluation criteria for each connection scenario include:

- ✓ Internal force distribution: analysis of variations in bending moments, shear forces, and stress distribution along main members;
- ✓ Deflection and local deformation: comparison of vertical displacements, joint rotations, and relative deformation between different configurations;

Critical load causing geometric instability: in cases where geometric nonlinearity is considered, analysis is carried out until the structure becomes unstable or reaches a critical load [10,11].

The integration of two computational strategies—using both commercial software and in-house coding—along with validation against published benchmarks [9,11], enhances the reliability of the outcomes and enables sensitivity studies on how structures respond to different connection placements. These findings provide a foundation for suggesting practical design guidelines applicable to modern steel frames incorporating semi-rigid joints.

A schematic diagram of the analysis workflow is presented below.

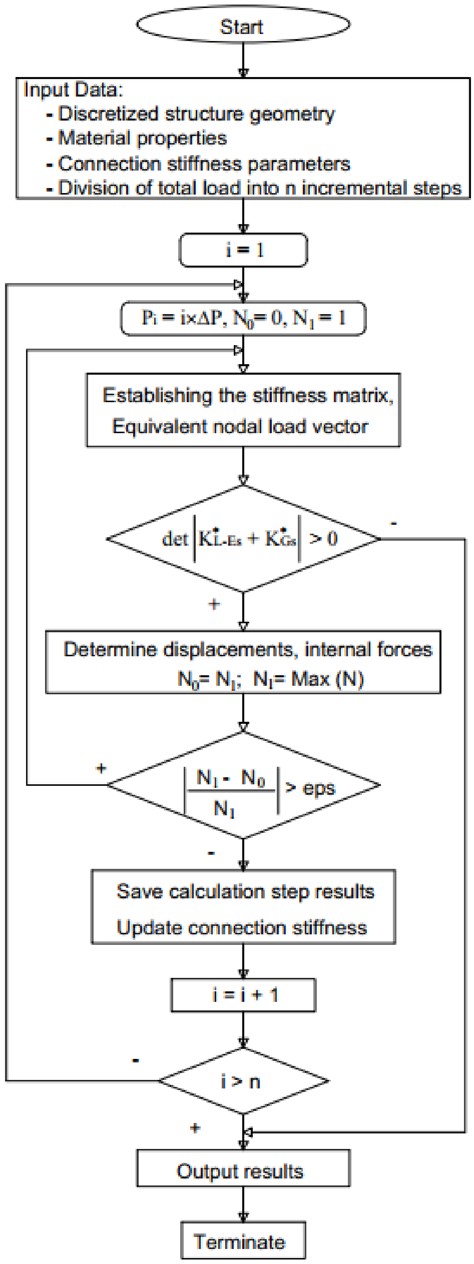

Fig. 2. Flowchart of step-by-step loading analysis for steel frames with semi-rigid connections.

Explanation of Figure 4 – Incremental Load Analysis Workflow

Figure 4 illustrates the flowchart of an incremental static loading procedure applied to steel frames incorporating nonlinear semi-rigid joints and accounting for geometric (P–Δ) effects. The procedure is described step by step below:

1. Start

   Initialization of the algorithm.

2. Input Data:

   Discretized structural geometry;

   Material properties;

   Semi-rigid connection stiffness parameters;

   Division of total load into incremental steps.

3. Initialize Analysis Variables:

   Load at step i: $P_i = i\Delta P$

   Previous iteration value $N_0 = 0$

   First iteration $N_1 = 1$

   Set initial load step index $i = 1$

4. Formulate the global stiffness matrix together with the corresponding equivalent nodal load vector.
5. Check for Structural Stability:

   If $det[K^*_{L-Es} + K^*_{Gs}] > 0$ the structure has not yet reached instability.

6. Solve for Displacements and Internal Forces:

   Compute displacements and internal forces;

   Update current load value $N_{new} = N_i$

   Determine the maximum nodal reaction $N_{ref} = (N)$

7. Convergence Check:

   If $\left|\frac{N_1 - N_0}{N_1}\right| > eps$ (convergence threshold),

   go back to update the connection and repeat the iteration.

8. Save Results for the Current Step:

   Revise the rotational stiffness of semi-rigid joints according to the specified moment–rotation law.

9. Increment Load Step:

   $i = i + 1$

   If $i > n$, proceed to output;

   Otherwise, continue to the next load step.

10. Output Results:

    Export final results for displacements, forces, and stability assessment.

11. Terminate:

    End of analysis.

Figure 4 presents the flowchart of the incremental static loading analysis for steel frames with semi-rigid connections and geometric nonlinearity. In this procedure, the total applied load was divided into 100 incremental steps (1% of the ultimate load per step), with a convergence tolerance of 10^{-3} based on the displacement norm.

It should be noted that SAP2000 only allows rotational springs to be assigned at element ends. To represent mid-span connections, the elements were subdivided and their stiffness calibrated according to the MATLAB formulation, ensuring consistency between the two platforms.

In this study, the "critical load" is defined as the elastic buckling load, determined when the determinant of the global stiffness matrix $[K_{L-Es}^{*} + K_{Gs}^{*}]$ becomes zero, which indicates the onset of instability.

4. Results and discussion

4.1. Verification of the element model using published benchmark problems

Example 1. Frame with Fully Rigid Connections – Verification of First- and Second-Order Elastic Analysis. To verify the reliability of the developed finite element formulation incorporating semi-rigid joints, a benchmark problem involving a two-story, single-bay steel frame reported in earlier studies [9,19–21] was recalculated. In this validation case, the beam–column connections are considered fully rigid. Each beam member is modeled with three elements, where the segment next to the column is taken as very short—equivalent to representing the joint at the element end, consistent with [9].

The loading conditions consist of a horizontal force H = 44.5 kN and a vertical force P = 444.8 kN. The structural material is steel specified according to AISC provisions, with an elastic modulus of E = 199,948 MPa. For the semirigid case, the column–beam joint was assigned a rotational stiffness of 88.889 kN·m/rad (786.732 kips·in/rad). The numerical model was developed in MATLAB, and its results were cross-checked against SAP2000 simulations and published benchmarks to ensure accuracy.

Figure 5. Validation model of a frame incorporating semi-rigid joints located at the beam mid-span (developed by the authors based on geometry and loading conditions in [9]).

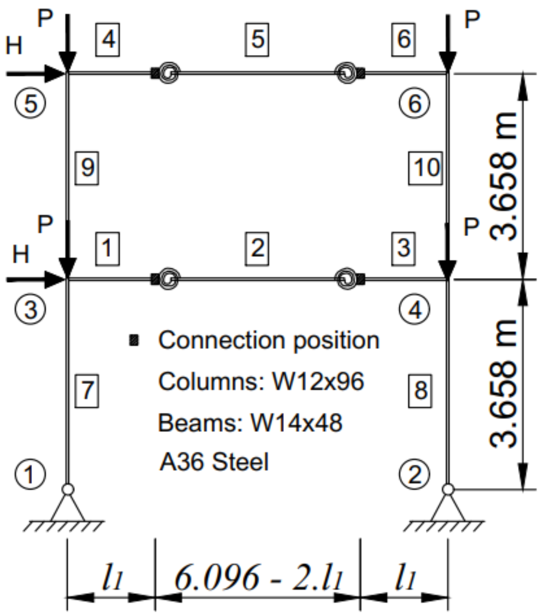

Fig. 5. Validation model of a frame incorporating semi-rigid joints located at the beam mid-span.

The benchmark problem originates from the experimental study of Stelmack (1982) [1], later adopted by Kim and Choi (2001) [22], involving a two-story, single-span steel frame subjected to concentrated static loading. The frame consists of W12 × 96 steel columns and W14 × 48 steel beams made of A36 steel, with pinned column bases. Semi-rigid beam–column connections were detailed using A325 bolts and L4 × 4 × 1/2 in angle cleats at the beam flanges. The applied vertical load (P_1 = 10.68 kN) was placed at the third points of the first-story beam, along with two proportional horizontal loads.The geometry of the verification frame model is illustrated in Fig. 5. Elements 1, 3, 4, 6, 9, and 10 are modeled with rigid connections at both ends. Elements 2 and 5 have semi-rigid connections at both ends, while elements 7 and 8 have one end modeled as rigid and the other as pinned.

In Figure 5, the parameter l_1 represents the length of the boundary elements (elements 1 and 3 on the lower story, and elements 4 and 6 on the upper story), corresponding to the distance from the support to the first semi-rigid connection along each beam. The length of the mid-span elements (elements 2 and 5) is determined as $6.096 - 2l_1$, ensuring that the total span length remains constant.

4.1.1. First-order elastic analysis

In this case, elements 2 and 5 are modeled with semi-rigid connections at both ends, but with infinite rotational stiffness. The calculated lateral displacements at critical nodes and the maximum bending moments are presented in Tables 1 and 2. The discrepancy between the proposed model and the reference studies is less than 0.2%, confirming the high accuracy of the developed formulation.

Table 1. Lateral displacement of the frame (mm).

Node #	Beam-end connection in the traditional model			l_1=0.01m	(B-A)/(A) (%)
	[19] (A)	[9]	SAP 2000	Present study (B)	
3	25.7	25.6896	25.691	25.6896	-0.04
5	38.3	38.3513	38.354	38.3513	0.13

Table 2. Maximum bending moments in structural members (kN·m).

Member #	Beam-end connection in the traditional model			l_1=0.01m	(B-A)/(A) (%)
	[19] (A)	[9]	SAP 2000	Present study (B)	
1, 3	163.8	163.8852	187.17	163.8852	0.05
4, 6	80.3	80.3692	89.81	80.3692	0.09
7	163.0	163.1010	189.57	163.1010	0.06
8	162.4	162.4610	188.7	162.4610	0.04
9	80.3	80.3224	89.76	80.3224	0.03

Note: In the traditional configuration, semi-rigid connections are placed directly at the beam–column joints (i.e., at the beam ends), corresponding to the case shown in Fig. 5 with l_1=0.01m. This setup is consistent with the configurations used in the reference studies

4.1.2. Second-order elastic analysis

When geometric nonlinearity (P–Delta effect) is considered, the analysis results are further compared, as shown in Tables 3 and 4. The discrepancies remain below 0.2%, demonstrating that the proposed model performs well even under geometrically nonlinear conditions.

Table 3. Lateral displacement with p–delta effect (mm).

Node #	Beam-end connection in the traditional model			l_1=0.01m	(B-A)/(A) (%)
	[19] (A)	[21]	[20]	Present study (B)	
3	29.7	29.6	29.7	29.689	-0.037
5	44.0	43.8	44.0	43.9818	-0.041

Table 4. Maximum bending moments with p–delta effect (kN·m).

Member #	Beam-end connection in the traditional model			l_1=0.01m	(B-A)/(A) (%)
	[19] (A)	[21]	[20]	Present study (B)	
1, 3	186.9	186.8	187.1	187.1927	0.157
4, 6	89.8	89.8	89.8	89.8144	0.016
7	189.5	189.4	189.5	189.5958	0.051
8	188.6	188.6	188.6	188.7185	0.063
9	89.7	89.7	89.7	89.7674	0.075
10	89.8	89.8	89.7	89.8144	0.016

4.1.3. Verification with semi-rigid connection at beam end

To validate the model under conditions where the connection is not perfectly rigid, a similar problem is formulated with a rotational stiffness of 88.889 kNm/rad at the beam ends. The results (Tables 5 and 6) continue to show very small errors (< 0.2%) when compared with the literature ([19], [21], [20]).

Table 5. Displacement – semi-rigid ends (mm).

Node #	Beam-end connection in the traditional model			l_1=0.01m	(B-A)/(A)
	[19] (A)	[21]	[20]	Present study (B)	(%)
3	37.5	37.4	37.5	37.5078	0.021
5	58.2	58.1	58.2	58.1768	-0.040

Table 6. Moments – semi-rigid ends (kN·m).

Member #	Beam-end connection in the traditional model			l_1=0.01m	(B-A)/(A)
	[19] (A)	[21]	[20]	Present study (B)	(%)
1, 3	184.6	184.6	184.8	184.90	0.163
4, 6	101.9	101.9	101.9	101.88	-0.015
7	196.5	196.4	196.5	196.56	0.029
8	195.6	195.5	195.7	195.67	0.035
9	101.9	101.9	101.8	101.84	-0.054
10	101.9	101.9	101.9	101.88	-0.015

Minor discrepancies between MATLAB and SAP2000 appeared in intermediate displacements, but after element subdivision and parameter tuning, the results converged with differences below 0.2% compared to published benchmarks.

4.2. Influence of semi-rigid connection placement on steel frame behavior

Example 2. Frame with Semi-Rigid Connections — Varying Connection Positions.

After validating the model using semi-rigid joints located at the beam–column ends, this study extends the investigation by maintaining the same frame layout while shifting the semi-rigid connections to the mid-span of beams or to the mid-height of columns. Under this modification, the lengths of the beam-end segments differ considerably, and thus no longer correspond to the short elements adjacent to the joints as described in Section 4.1.

Table 7 presents the variation in lateral displacement at Nodes 3 and 5 as the position of the semi-rigid connection shifts along the beam span—from near the joint (l_1 = 0.01 m) to the mid-span (l_1 = 2.5 m). The results indicate:

Table 7. Displacement – mid-span connection (mm).

Node #		l_1=0.01m	l_1=0.5m	l_1=1m	l_1=1.5m	l_1=2m	l_1=2.5m
3	Displacement (mm)	37.5078	35.1676	33.2198	31.7038	30.6123	29.9416
	% change	-	-6.23%	-11.45%	-15.48%	-18.38%	-20.17%
5	Displacement (mm)	58.1768	53.8987	50.3555	47.6105	45.6416	44.4353
	% change		-7.35%	-13.44%	-18.12%	-21.56%	-23.63%

- ✓ A consistent reduction in displacement as the connection moves away from the joint toward the beam's center.
- ✓ At Node 3, the displacement decreases from 37.5 mm to 29.9 mm, representing a reduction of nearly 20%.
- ✓ This trend demonstrates that placing connections in regions with lower bending moments (mid-span) enhances the global stiffness of the frame, reduces lateral deformation, and improves structural stability.

Table 8 presents the bending moments in key structural members as the connection position varies:

Table 8. Moments – mid-span connection (kN·m).

Member #		l_1=0.01m	l_1=0.5m	l_1=1 m	l_1=1.5m	l_1=2m	l_1=2.5m
1, 3	Moment (kN·m)	184.90	185.28	185.77	186.29	186.74	187.07
	% change	–	+0.21%	+0.47%	+0.75%	+1.00%	+1.17%
4, 6	Moment (kN·m)	101.88	98.57	95.63	93.21	91.40	90.25
	% change	–	-3.25%	-6.14%	-8.52%	-10.28%	-11.49%
7	Moment (kN·m)	196.56	194.47	192.74	191.39	190.41	189.81
	% change	–	-1.06%	-1.94%	-2.64%	-3.13%	-3.43%
8	Moment (kN·m)	195.67	193.59	191.86	190.51	189.54	188.95
	% change	–	-1.06%	-1.94%	-2.64%	-3.13%	-3.44%
9	Moment (kN·m)	101.84	98.53	95.59	93.17	91.36	90.21
	% change	–	-3.25%	-6.14%	-8.49%	-10.30%	-11.47%
10	Moment (kN·m)	101.88	98.57	95.63	93.21	91.40	90.25
	% change	–	-3.25%	-6.14%	-8.52%	-10.28%	-11.49%

- ✓ Members near the joints (e.g., Members 1, 3; 4, 6; 9, 10) show a decreasing trend in moment as the connection is moved outward, indicating a reduction in stress concentration at the joints.
- ✓ Conversely, mid-span members (e.g., Members 7 and 8) show stable or slightly increasing moments, reflecting a more balanced redistribution of internal forces along the beam.
- ✓ Overall, the results demonstrate an effective reallocation of internal forces, contributing to a more uniform and efficient structural performance.

Example 3. Two-Story, One-Bay Steel Frame Incorporating a Semi-Rigid Joint at Mid-Span (Position P1).

This example is based on the experimental configuration described in [9], which was previously used by Kim and Choi [22] to validate a nonlinear semi-rigid connection model. The two-story, single-span steel frame shares the same geometry, loading, and boundary conditions as the published model, allowing for direct comparison of connection placement strategies.

In this work, rather than placing the semi-rigid joint at the beam–column intersection as in earlier studies, it is assigned to the mid-span of the first-story beam (denoted as Position P1). This configuration simulates practical construction scenarios in which beams are divided for transportation and later assembled on site. At Position P1, the joint rotational stiffness is represented through the Kishi–Chen [9] three-parameter model, providing an accurate description of its nonlinear moment–rotation response.

The structural frame is analyzed using beam–column elements incorporating semi-rigid joints and accounting for geometric nonlinearity (P–Δ effect). Material nonlinearity is neglected in this study, as the steel members are assumed to remain in the elastic range up to the critical load. The primary objective is to investigate the influence of semi-rigid connection placement on static stability, where geometric nonlinearity plays the dominant role. Numerical simulations are carried out in MATLAB, and the obtained results are benchmarked against previously reported load–displacement curves at the first-story level ([9], [22]), thereby validating the model and assessing the influence of joint placement.

Figure 6. Validation model of a two-story, one-bay steel frame with a mid-span semi-rigid connection (Position P1), redrawn by the authors based on geometry and loading conditions in [9].

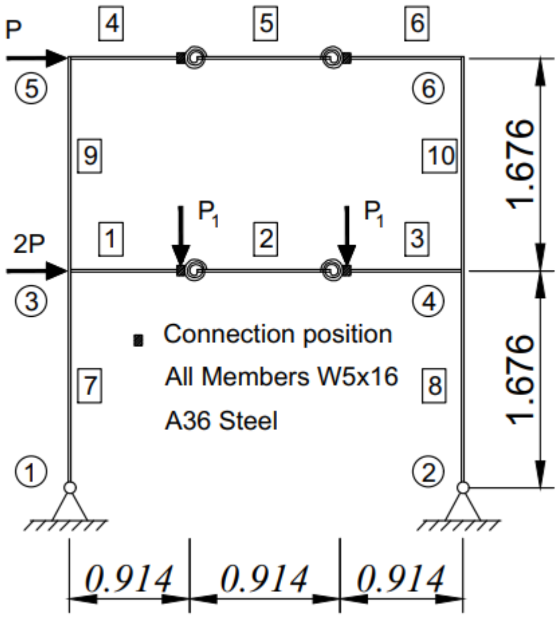

Fig. 6. Validation model of a two-story, one-bay steel frame with a mid-span semi-rigid connection (Position P1, where a semi-rigid joint is introduced at the beam mid-span).

The benchmark model is based on the experimental study of Stelmack (1982) [2], later adopted by Kim and Choi (2001) [22] and Chan & Chui [2]. It consists of a two-story, single-span steel frame fabricated with W12 × 96 steel columns and W14 × 48 steel beams using A36 steel according to AISC provisions. The column bases are pin-supported, and semi-rigid beam–column connections were realized with A325 bolts and L4 × 4 × 1/2 in angle cleats at the beam flanges. The applied vertical load (P1 = 10.68 kN) was placed at the third points of the first-story beam, combined with two proportional horizontal forces.

The structural response is validated against the experimental results in terms of horizontal load–displacement and moment–rotation at the connections. The nonlinear behavior of the semi-rigid joints is represented by the Kishi–Chen exponential model [9], with key parameters: initial stiffness k_0 = 3373.16 kN·m/rad (29855 kips·in/rad), ultimate moment Mu = 20.90 kN·m (185 kips·in), and shape factor n = 1.65. The numerical simulations were carried out in MATLAB and compared with published benchmarks, with results presented in Figures 6 and 7.

Figure 6 depicts the load–displacement curve at the first story of a two-story, one-bay steel frame in which a semi-rigid joint is positioned at the mid-span (Position P1).

The results from the present model (red curve) are compared with the experimental data from [9] and the numerical models in [22]. The computed response exhibits a clearly nonlinear trend and reaches a significantly higher critical load—approximately 40 kN greater—than the referenced studies. This discrepancy highlights the positive impact of redistributing the connection location, which enhances the overall stiffness and stability of the structure.

The numerical analysis shows that placing the semi-rigid connection at the mid-span (Position P1), instead of at the beam end, significantly improves the frame's structural performance:

Bending moments near the joints are substantially reduced, while the moment in the mid-span region increases in a reasonable manner, reflecting a more uniform internal force distribution along the beam. This helps alleviate stress concentration at joints, which are typically weak points susceptible to failure.

Lateral displacement at the first story decreases as the length of the beam-end segment increases. Specifically, when this length increases from 0.01 m to 2.5 m, the displacement at Node 3 decreases from 37.5 mm to approximately 29.9 mm—an impressive result that confirms the beneficial effect of changing connection placement while fully accounting for geometric nonlinearity.

The analysis results reveal significant differences:

As illustrated in Fig. 7, the load–displacement curve at the first story of the steel frame with a mid-span semi-rigid connection demonstrates a significant improvement in load-bearing capacity. Specifically, the elastic critical load in the present model reaches nearly 40 kN, whereas the value reported by Kim and Choi [22] is only approximately 12 kN. All curves in Fig. 7 were generated by the authors using MATLAB simulations, with experimental reference values from [9], [22] employed solely for validation.

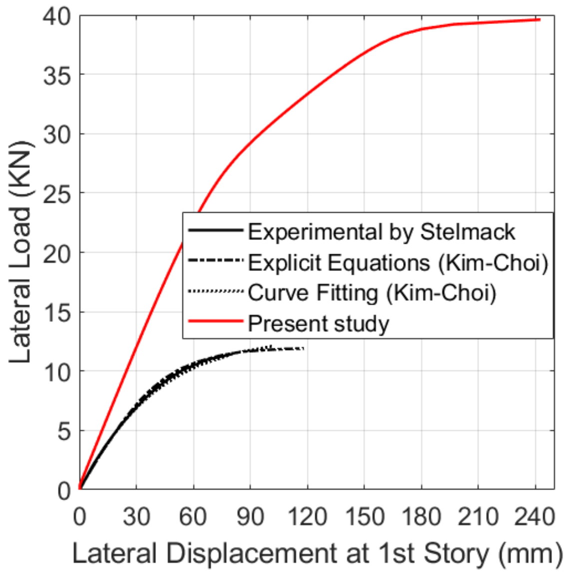

Fig. 7. Load–displacement curve at the first story of the steel frame with a mid-span semi-rigid connection (Position P1, located at the beam mid-span). All curves were generated by the authors using MATLAB simulations, with experimental reference values from [9], [22] employed solely for validation.

Thus, the configuration with the semi-rigid connection placed at the mid-span of the beam can increase the critical load capacity by over 230%, equivalent to more than three times that of the traditional connection model.

This enhancement mechanism can be explained as follows: In the traditional model, the semi-rigid connection is located at the beam–column joint, where the bending moment is typically the highest. Consequently, the rotational stiffness of the connection is highly mobilized, significantly reducing the overall structural stiffness. In contrast, in the proposed model, the semi-rigid connection is relocated to the mid-span of the beam—where the bending moment is much smaller—so the negative impact on the global stiffness is minimal. As a result, the structure is able to maintain higher stiffness and achieves a much greater critical load.

These results clearly demonstrate the significant influence of connection placement on internal forces, deformations, and geometric stability of the frame. This provides an important design insight that should be seriously considered in structures where members are segmented for practical on-site assembly.

4.3. Technical discussion and design recommendations

From the two verification scenarios above, several practical conclusions can be drawn:

- ✓ The simplified model (connection at joint) is only appropriate when the element is very short, representing the case of a connection located at the beam or column end.
- ✓ In cases where the connection is placed at the mid-span of a beam or mid-height of a column, detailed modeling using elements with semi-rigid connections is essential to accurately capture the structural behavior.
- ✓ Practical design implication: In structures where members must be segmented for transportation and assembly, mid-span or mid-column connections are common and must be thoroughly considered in the design process. In addition, members with variable stiffness such as tapered or haunched beams may further optimize the benefits of mid-span connections by redistributing bending moments more effectively. This represents a promising direction for future applications.

5. Limitations and future work

Despite the significant findings presented in this study, several limitations should be acknowledged to guide future research:

- ✓ The analysis is limited to static loading conditions; dynamic or cyclic loading scenarios, which may influence fatigue and long-term stability, were not considered.
- ✓ The current study focuses on planar frames with constant material and cross-sectional properties. Extension to space frames or tapered sections would enhance practical relevance. Current design codes such as AISC primarily address end-joint connections and do not explicitly consider non-traditional internal joints. The present findings highlight the need for future revisions or supplementary guidelines to accommodate mid-span or tapered-member connection layouts, supported by additional experimental validation.
- ✓ The uncertainties in material properties, connection stiffness, and construction tolerances were not incorporated, though these can affect real-world behavior.
- ✓ The investigation considers a limited set of connection positions, primarily near the mid-span of the first-story beams. Broader exploration of possible connection locations could provide a more comprehensive understanding.
- ✓ Future studies may benefit from incorporating dynamic analysis, reliability-based methods, and experimental validation to further improve the robustness and applicability of the proposed modeling approach.
- ✓ This study is limited to planar steel frames with constant cross-sections. Nevertheless, the observed trends regarding the influence of semi-rigid connection placement on stability are expected to remain qualitatively valid for more complex configurations, such as three-dimensional frames or frames with tapered sections. Future investigations will extend these scenarios to confirm the generality of the findings.
- ✓ While the present analysis focuses on static loading conditions, it is worth emphasizing that semi-rigid connections contribute significantly to ductility and energy dissipation—factors that are critical under dynamic or seismic excitations. Future work will extend the framework to dynamic and seismic loading scenarios to further enhance the practical relevance of the results.
- ✓ Nevertheless, the quantitative level of improvement observed in static cases may vary under cyclic or seismic loading, as joint ductility and potential degradation mechanisms become more influential. Future studies will therefore investigate the role of mid-span connections in dynamic performance to confirm the generality of the conclusions.

- ✓ The present results were obtained for single-span planar frames under symmetric loading. While the beneficial effect of mid-span connections is expected to remain qualitatively valid in multi-span frames or under asymmetric loading, the quantitative improvement in critical load may differ. Future studies will extend the analysis to these cases.
- ✓ The present analysis was conducted for beams and columns with fixed sectional properties. Although the absolute values of displacement will vary with different beam slenderness ratios or column stiffnesses, the qualitative trend of reduced lateral displacement when connections shift toward mid-span is expected to remain valid. Future studies will parametrize these effects to confirm the generality of the findings.
- ✓ The present model assumes idealized connections without construction tolerances or bolt slippage. In real prefabricated assemblies, these factors may reduce the effective rotational stiffness and slightly diminish the predicted stability improvement. Future experimental and probabilistic studies are needed to quantify their influence.

6. Conclusions

This paper has presented a numerical study analyzing the influence of semi-rigid connection placement on the static behavior of planar steel frames, using a finite element model that incorporates geometric nonlinearity (P–Delta effect). Unlike most existing studies, which focus primarily on connections located at beam–column joints, this research expands the investigation to include alternative configurations such as mid-span or mid-height connections and distributed connections along the member length—reflecting modern construction practices where structural elements are often segmented for transportation and on-site assembly.

Three semi-rigid connection placement scenarios were analyzed:

- ✓ Connections located at the ends of beams or columns (traditional configuration);
- ✓ Connections placed at the mid-span of beams or mid-height of columns;
- ✓ Connections distributed uniformly along the length of the member.

The simulation results reveal the following key findings:

- ✓ More favorable internal force distribution is achieved when connections are placed at mid-span or mid-height. Bending moments at joints are reduced by up to 30%, while internal forces at mid-segments increase slightly and become more stable, helping to reduce stress concentration and the risk of local failure.
- ✓ Lateral displacement of the frame does not increase as commonly expected. On the contrary, it tends to decrease slightly as the length of the beam-end segment increases. This reflects an improvement in stiffness distribution and a more uniform structural response.
- ✓ Elastic critical load increases significantly: the model with mid-span semi-rigid connections reaches a critical load of nearly 40 kN—more than 230% higher than the approximately 12 kN reported in previous studies such as [22]. This demonstrates a clear enhancement in global stability when connection placement is optimized.
- ✓ High practical applicability: Placing connections at mid-span or mid-height enables segmentation of structural members, reduces transportation costs, and facilitates on-site construction, all while maintaining or improving overall structural stability.

Based on these findings, the authors recommend that current steel frame design methods broaden their modeling scope beyond traditional joint-based connections. Internal semi-rigid connections located along the member length should be more thoroughly studied, integrated into design procedures, and standardized, in order to fully harness the load-bearing potential of structural systems under increasingly diverse construction conditions.

Funding

The author received no financial support for the research, authorship, or publication of this article.

Conflict of Interest

The author declares no conflict of interest.

References

[1] Zhao H, Liu X-G, Tao M-X. Component-based model of semi-rigid connections for nonlinear analysis of composite structures. Eng Struct 2022;266:114542. https://doi.org/10.1016/j.engstruct.2022.114542.

[2] Chan SL, Chui PPT. Non linear static and cyclic analysis of steel frames with semi rigid connections. Amsterdam: Elsevier; 2000.

[3] Kılıç M, Sagiroglu M, Maali M, Cüneyt A. Experimental and numerical investigation of semi-rigid behavior top and seat T-Section connections with different triangular designed stiffener thicknesses. Eng Struct 2023;289:116216. https://doi.org/10.1016/j.engstruct.2023.116216.

[4] Lu S, Wang Z, Pan J, Wang P. The Seismic Performance Analysis of Semi-rigid Spatial Steel Frames Based on Moment-Rotation Curves of End-plate Connection. Structures 2022;36:1032–49. https://doi.org/10.1016/j.istruc.2021.12.064.

[5] Fathizadeh SF, Dehghani S, Yang TY, Vosoughi AR, Noroozinejad Farsangi E, Hajirasouliha I. Seismic performance assessment of multi-story steel frames with curved dampers and semi-rigid connections. J Constr Steel Res 2021;182:106666. https://doi.org/10.1016/j.jcsr.2021.106666.

[6] Masoumi A, Preciado A. Experimental and analytical investigations of enhanced semi-rigid connections with dual pipe dampers. Structures 2021;33:3765–78. https://doi.org/10.1016/j.istruc.2021.06.106.

[7] Zhai X, Zha X, Wang K, Wang K, Wang H. Shake table tests of a full-scale two-story plate-type modular composite building with semi-rigid corner connections. Eng Struct 2023;289:116325. https://doi.org/10.1016/j.engstruct.2023.116325.

[8] Pirchio D, Pozo JD, Walsh KQ. Adhered web-lapped semi-rigid pultruded FRP beam-to-column framing connections: Part 1 – Experimental study. Compos Part B Eng 2025;292:112059. https://doi.org/10.1016/j.compositesb.2024.112059.

[9] Vu QA, Dung BT Le, Nguyen HQ. Shape Functions Development for Beam-Column Element with Semi-Rigid Connections in Second-Order Steel Frame Analysis. Civ Eng J 2025;11:369–92. https://doi.org/10.28991/CEJ-2025-011-01-021.

[10] Wang Q, Su M. Stability study on sway modular steel structures with semi-rigid connections. Thin-Walled Struct 2021;161:107529. https://doi.org/10.1016/j.tws.2021.107529.

[11] Vu QA, Nguyen HQ, Lê, Bao DLT. FEM-based prediction of elastic critical loads in steel frames with nonlinear semi-rigid connections. J Mater Constr 2025;15:38–44. https://doi.org/10.54772/jomc.v15i01.960.

[12] Ibrahimov K, Sabbagh AB, Jafarifar N, Davidson P. Experiments on cyclic behaviour of reusable side plate cold-formed steel semi-rigid moment-resisting connections. Eng Struct 2025;341:120797. https://doi.org/10.1016/j.engstruct.2025.120797.

[13] Zhai X, Zha X, Wang K, Wang H. Initial lateral stiffness of plate-type modular steel frame structure with semi-rigid corner connections. Structures 2023;56:105021. https://doi.org/10.1016/j.istruc.2023.105021.

[14] Wang X, Lu G, Liu Y, Chen Z, An Q, Wang X. Lateral stiffness of modular steel joint with semi-rigid bolted intra-module connection. J Build Eng 2024;97:110668. https://doi.org/10.1016/j.jobe.2024.110668.

[15] Du B, Jiang W, He Z, Qi Z, Zhang C. Development of a modified low-cycle fatigue model for semi-rigid connections in precast concrete frames. J Build Eng 2022;50:104232. https://doi.org/10.1016/j.jobe.2022.104232.

[16] Wu Z, Lu X, Bao H, Li L, Lu Z. Experimental response of semi-rigid reinforced concrete beam-column joints with bolted angle dissipating connections. J Build Eng 2024;90:109345. https://doi.org/10.1016/j.jobe.2024.109345.

[17] Moghaddam H, Sadrara A. Improving the mechanical characteristics of semi-rigid saddle connections. J Constr Steel Res 2021;186:106917. https://doi.org/10.1016/j.jcsr.2021.106917.

[18] Lee S, Lee J, Seo B, Kim D, Kim D, Jo Y. Stiffness evaluation of semi-rigid connection using steel clamps in plastic greenhouse structure. Biosyst Eng 2025;250:15–27. https://doi.org/10.1016/j.biosystemseng.2024.11.018.

[19] Kim S, Choi S. Practical advanced analysis for semi-rigid space frames. Int J Solids Struct 2001;38:9111–31. https://doi.org/10.1016/S0020-7683(01)00104-X.

[20] Bhatti HJD. Effects of connection stiffness and plasticity on the service load behavior of unbraced steel frames. Eng J 1995;32:21–33.

[21] Dhillon BS, O’Malley III JW. Interactive design of semirigid steel frames. J Struct Eng 1999;125:556–64.

[22] C. Y. Abolmaali. Nonlinear moment reversal behavior in steel frames. Korean Sci J 2004;5:3–15.